SUPPORTING INFORMATION

The C34 peptide fusion inhibitor binds to the 6-helix bundle core domain of HIV-1 gp41 by displacement of the C-terminal helical repeat region

John M. Louis*, James L. Baber and G. Marius Clore*

Laboratory of Chemical Physics, National Institute of Diabetes and Digestive and Kidney Diseases, National Institutes of Health, DHHS, Bethesda, Maryland 20892-0520

5 Figures

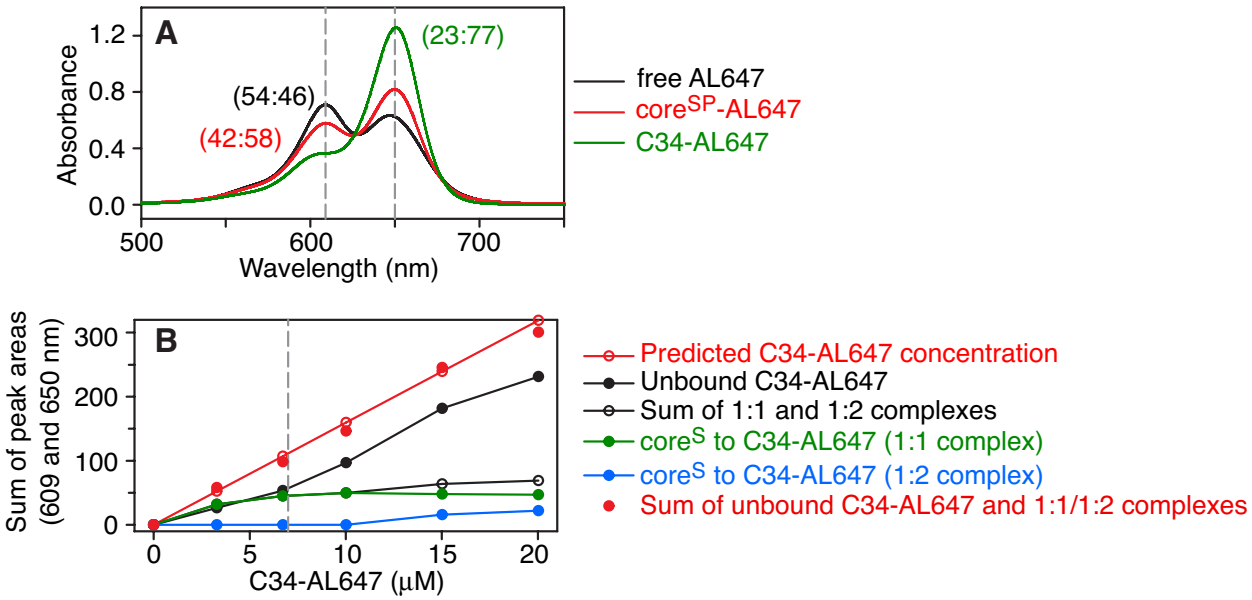

Figure S1. Properties of AL-647 dye. (A) Effect of AL647 proximity to other AL647 molecules on its relative absorbance at 609 and 650 nm. When not in close proximity to other dye moieties, as in the case of C34-AL647 (green trace) which does not self-associate, AL647 exhibits minimal absorbance at 609 nm relative to 650 nm. The peak at 609 nm markedly increases relative to 650 nm when intermolecular proximity between AL647 moieties is increased as expected in core^{SP}-AL647 (red trace) owing to 6-HB formation (see Fig. 1D). Note that excess unreacted AL647 (free AL647, black trace) recovered from the column exhibits self-association. Relative ratios of absorbance at 609 and 650 nm are indicated in parentheses beside the traces. (B) Preliminary quantitative binding data of C34-AL647 to the core^{S} trimer. Open red circles represent the projected sum of absorbance at 609 and 650 nm based on a standard injection of C34-AL647. Solid black, green and blue circles represent peak areas of free C34-AL647 and its 1:1 and 2:1 complexes with core^{S} trimer, respectively, similar to that shown in Fig. S3. Open black circles correspond to the sum of the absorbance of 1:1 and 2:1 complexes (values of closed green + closed blue circles). These values added to that of free C34-AL647 at each given concentration are shown as solid red circles. The consistency between the input quantities and the sum of the observed peak areas validates the method used to quantify the concentrations of the complexes based on AL647 absorbance. Equimolar ratio of core^{S} (as monomer) and C34-AL647 is shown by the vertical dashed gray line.

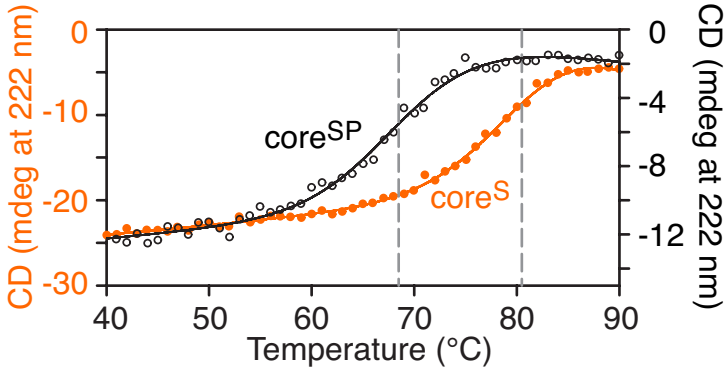

Figure S2. Thermal melting of core^{S} and core^{SP} in 10 mM Tris-HCl, pH 7.6, 150 mM NaCl (buffer A). Traces of the 222 nm CD signal of core^{S} (red, 3.8 µM) and core^{SP} (black, 2.5 µM) as a function of increasing temperature.

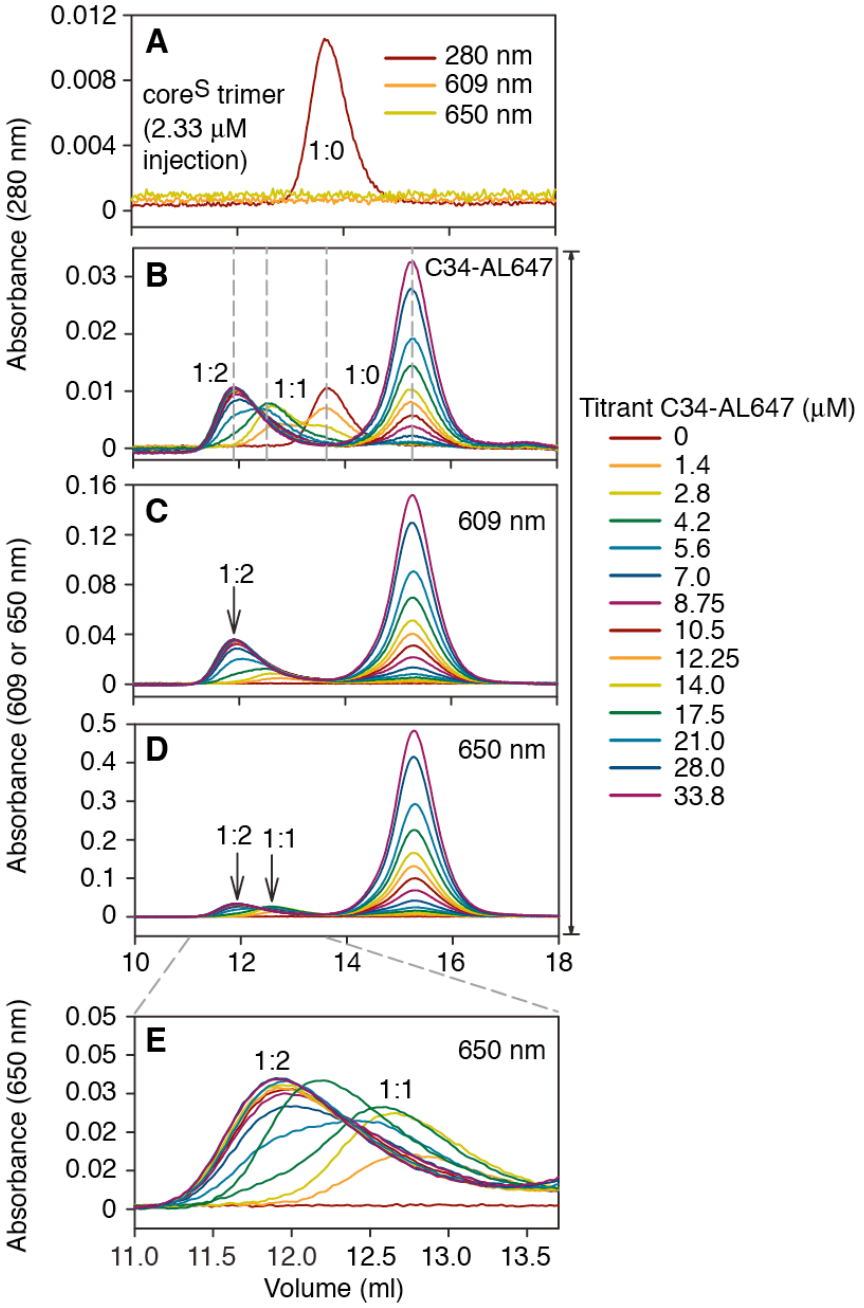

Figure S3. SEC profiles obtained upon titrating C34-AL647 into core^S trimer. Increasing concentrations of C34-AL647 (1.4-33.8 µM) were added to unlabeled 2.33 µM core^S trimer in a total injection volume of 100 µl. (*A*) Standard injection of core^S. (*B-D*) Progressive core^S /C34-AL647 complex formation as a function of increasing C34-AL647 concentration monitored at 3 wavelengths. C34-AL647 elutes at 15.5 ml, core^S at 13.7 ml, and core^S with one and two C34-AL647 peptides bound to it elute at ~12.6 and ~11.9 ml, respectively. The combined core^S/C34-AL647 bound forms were estimated by comparison with a standard injection of C34-AL647 alone based on the sum of the absorbance at 609 and 650 nm specific to

the AL647 dye (see Figure S1). (E) Enlarged view of (D) showing the transition from the 1:1 to the 1:2 complexes of core^{S}/C34-AL647 with increasing concentration of C34-AL647.

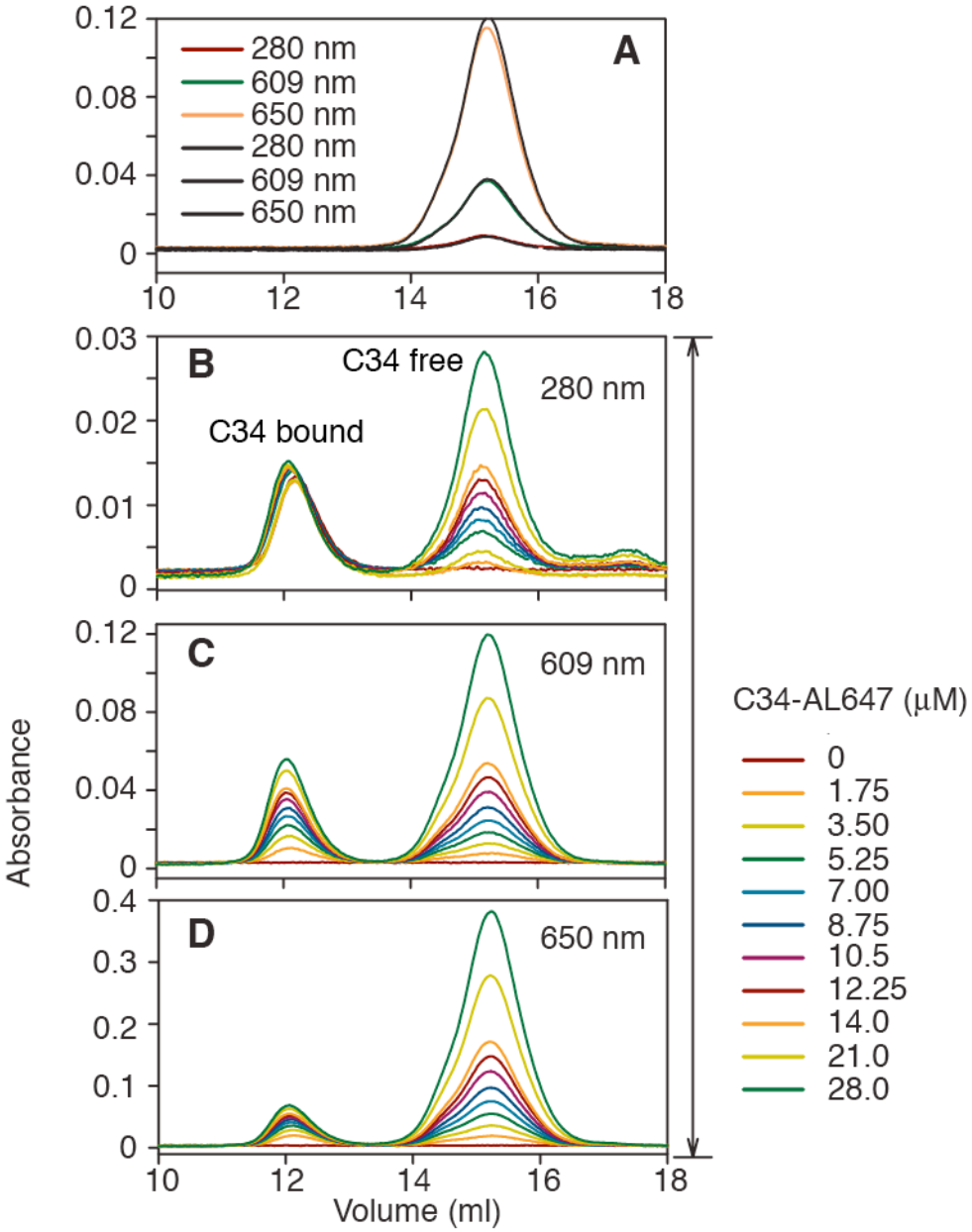

Figure S4. Size exclusion chromatography profiles obtained upon titrating C34-AL647 into unlabeled core^{SP} trimer. Increasing concentrations (1.75-28 μM) of C34-AL647 were added to 2.33 μM unlabeled core^{SP} trimer in a total injection volume of 100 μl. (A) Standard (duplicate) injections of 7 μM C34-AL647. (B-D) Progressive core^{SP}/C34-AL647 complex formation as a function of increasing C34-AL647 concentration monitored at 3 wavelengths. C34-AL647 elutes at 15.5 ml and 1:1, 1:2 and 1:3 complexes of C34-AL647 bound to the N-HR trimer from core^{SP} elute at ~12 ml.

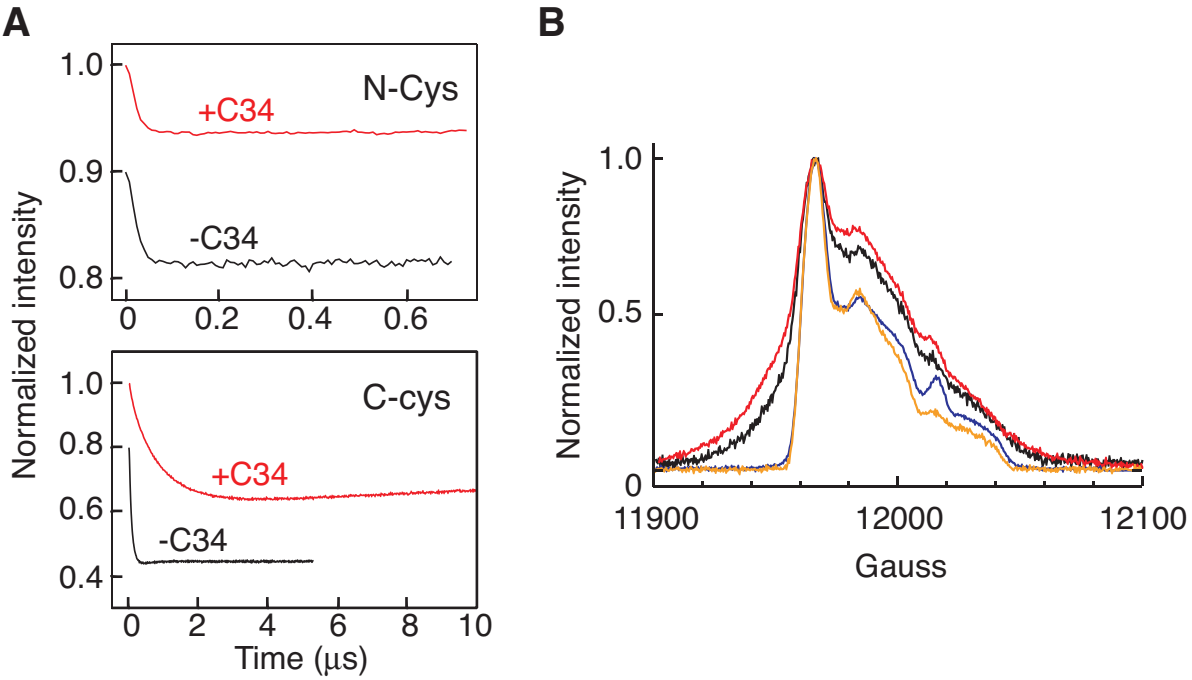

Figure S5. EPR DEER of fully deuterated, nitroxide-labeled core^{S} N-Cys and C-Cys constructs in the presence and absence of C34 peptide. The samples comprise 50 μM (in monomer units) core^{S} constructs with a 1.2 fold-excess per monomer of C34 (i.e. a molar ratio of 3.6:1 C34 to core^{S} trimer). (A) Background corrected DEER dipolar evolution curves used to calculate the P(*r*) distance distributions shown in Figure 5 of the main text. Red and black curves represent data acquired with and without C34 peptide, respectively. Note that the apparent modulation depth has been scaled relative to the raw data by the Ghost Suppression (for 3 spins) function of DeerAnalysis2013.[S1] (B) Normalized echo-detected field spectra. Red and black spectra were collected for the core^{S} N-Cys construct with and without C34 peptide, respectively. Orange and blue spectra were collected for the core^{S} C-Cys construct with and without C34 peptide, respectively. As the spectrometer was tuned to slightly different frequencies for the different samples, the actual abscissa of each spectrum was adjusted slightly (a few gauss) to facilitate comparison. A Hahn echo with 12 ns π/2 and 24 ns π pulses, a half-echo period of 400 ns, and an integration window of 80 ns was used to collect this data. All experiments were performed at a temperature of 50 K immediately prior to collection of the DEER data shown in Figure 5 of the main text. In the case of the core^{S} N-Cys data, significant broadening of the echo-detected field spectra (Fig. S5B) and severe attenuation of modulation depths (16 and 12% for free- and C34 bound, respectively; top panel in Fig. S5A), despite high labeling efficiency (>95%, based on electrospray ionization mass spectrometry, suggests the presence of a significant number of intersubunit spin-spin distances that are too close (< 15 Å) to measure by DEER. Consequently, the P(*r*) distributions for core^{S} N-Cys shown in Fig. 5A may be somewhat distorted by under-representation of spin-spin distances less than 15 Å. This has no bearing on the conclusions since addition of C34 has essentially no effect on the DEER data for core^{S} N-Cys.

References

S1. Jeschke, G., Chechik, V., Ionita, P., Godt, A., Zimmermann, H., Banham, J., and Timmel, C. R. (2006) DeerAnalysis2006 - a comprehensive software package for analyzing pulsed ELDOR data, *Appl.Magn.Reson. 30*, 473-498.